Stony Brook University

Breath biomarkers detection by chemical sensors

A Thesis Presented

by

Yan Li

to

The Graduate School

in Partial Fulfillment of the

Requirements

for the Degree of

Master of Science

in

Materials Science and Engineering

Stony Brook University

May 2015

Stony Brook University

The Graduate School

Yan Li

We, the thesis committee for the above candidate for the

Master of Science degree, hereby recommend

acceptance of this thesis.

Dr. Pelagia-Irene (Perena) Gouma
Professor, Department of Materials Science and Engineering

Dr. Dilip Gersappe
Professor, Department of Materials Science and Engineering

Dr. Jonathan Sokolov
Professor, Department of Materials Science and Engineering

This thesis is accepted by the Graduate School

Charles Taber
Dean of the Graduate School

Abstract of the Thesis

Breath biomarkers detection by chemical sensors

by

Yan Li

Master of Science

in

Materials Science and Engineering

Stony Brook University

2015

Our breath is a very complex mixture of chemical compositions. Usually, the majority of our exhaled breath consists of nitrogen, oxygen, carbon dioxides, water and inert gases. The remaining small fraction of breath contains thousands of components in trace amount, including inorganic gas molecules like nitric monoxide and diverse kinds of volatile organic compounds (VOCs). The concentrations of our exhaled gases are at a relatively stable level, though minor fluctuations may occur at different time of the day and they are also linked to the body status. Sometimes, if a specific breath gas of some appears to have an abnormal concentration, then it may be a hint that the person is ill. This breath gas therefore provide information of the healthy status of the body and is so-called biomarker.

Breath gases have long been used for diagnosis of disease by ancient Greek physicians centuries ago, the foundation of modern breath analysis, however, was established by Nobel Prize winner Linus Pauling in 1971. Though thousands kinds of gases exist in our exhaled breath,

only very limited number of them were confirmed by researchers to have a relatively strong linkage to some diseases and become biomarkers. Among all those biomarkers, nitric oxide, acetone and isoprene are the most studied. NO is believed to be in higher concentration in asthmatic patients breath. Acetone concentration is in elevated level in the breath of patients with diabetes. Isoprene is found to be related to cholesterol synthesis in our body.

Many techniques have been investigated to detect the existence of biomarkers. Spectroscopy-based techniques are highly accurate in detection of those biomarkers. The tradeoffs are that these devices are very expensive and bulky. In recent years, researchers have been developing chemical sensors mounted on breathalyzers to provide a real-time, non-invasive way for monitoring the concentration levels of breath. Compared to those spectroscopy-based devices, breathalyzers are low in cost, portable, painless and fast in response.

In this work, the chemical sensors for NO, acetone and isoprene detection are introduced. The chemical sensors can be divided into several groups based on the output signal. The most common group, chemiresistive sensors, is introduced in detail. In the experiment section, sensor is prepared with γ+ε-WO_3 as sensing material and its sensing properties to analyte gases like acetone, isoprene have been tested at different working temperatures. The results showed that the sensor was sensitive to acetone to some extent. However, it also exhibited selectivity to NO due to a coexistence of γ-WO_3 and ε-WO_3. Therefore, in order to improve the performance of this sensor, elimination of γ-WO_3 will be a possible way.

Table of Contents

List of Figures

List of Tables

Acknowledgments

It's not easy to write a thesis and I'm really grateful to those who helped me. Without your help and encourage, it would be impossible for me to finish this thesis.

First, I'd like to give my greatest appreciation to my advisor, Prof. Pelagia-Irene (Perena) Gouma. I'm really honored to have the opportunity to join her group and work on this promising and interesting topic. Thanks for all the instructions and advices she gave to me, which benefit me a lot.

Second, I'd like to thanks Prof. Dilip Gersappe and Prof. Jonathan Sokolov for serving as my thesis committee and I appreciate their recommendation for the acceptance of this work.

Then, I'd like to thank all my lab mates, Jusang Lee, Jiahao Huang, Wenling Liao, Gagan Jodhani, Selda Topcu, Chao Han and Xiecheng Jia for their help and advices. It's been a great time working with them in our lab.

Also, I'd like to acknowledge the support from the following grants for my thesis: NSF: Ⅱ-1231761.

Finally, special thanks must be given to my beloved parents. Without their support, it would be impossible for me to have the opportunity to study abroad and touch the world with different cultures.

Chapter 1 Introduction

1.1 Biomarkers in exhaled breath

Human breath is a very complex mixture of chemical compositions. Usually, the majority part of our exhaled gases consists of nitrogen, oxygen, carbon dioxides, water and inert gases. The remaining small fraction of breath contains thousands of components in trace amount, including inorganic gas molecules like nitric monoxide and diverse kinds of volatile organic compounds (VOCs). A series of nonvolatile substances such as peroxynitrite can also be found [1].

Though a large number of VOCs and other gases are ever detected in human breath, only a very limited number of them have the potential to be used for clinical diagnosis of diseases. These gases are the so-called biomarkers.

Biomarkers can be defined as "A characteristic that is objectively measured and evaluated as an indicator of normal biological processes, pathogenic processes, or pharmacologic responses to a therapeutic intervention [2]." A biomarker can be a substance whose existences or changes in concentration indicates the health status or severity of disease state of a person. Biomarkers can be specific cells, molecules, or genes, gene products, enzymes, or hormones.

1.1.1. NO in human breath

Exhaled nitric oxide is an endogenously produced gaseous molecule found in our breath. It is generated by three NO synthase: neuronal NOS, endothelial NOS and inducible NOS [3]. Exhaled NO has long been regarded as a biomarker for diagnosis of asthma. The concentration

of NO in a patient with asthma is usually higher than that of a healthy person. In some works [4, 5], researchers have found a cutoff value (NO>15 ppb) of NO for asthma, the predictive accuracy could be higher than 90%.

1.1.2 Two major VOCs in human breath

In 1971, Linus Pauling et cl detected more than 200 VOCs in breath and urine vapor by using gas chromatography (GC) [6]. His research was also commonly recognized as the foundation of modern breath analysis. In more recent work, researchers have identified more than 3000 VOCs. About 200 of them are widely detected in almost all breath samples, while the existence of others varies from individuals to individuals [7].

Acetone in human breath

As mentioned above, there are thousands of volatile organic compounds (VOCs) contained in human breath. Among all those VOCs, breath acetone is one of the most abundant one in our exhaled breath. Acetone is generally regarded as a biomarker for diagnosis of diabetes. Diabetic patients typically have higher concentration of exhaled acetone and this may result in a sweet odor in their breath [8]. For most VOCs, the measured values in human breath vary a lot. This may due to the variability between (and within) individuals as well as from the sampling and analysis methods. In Ref. [9], the concentration range of acetone was summarized and it lied in 1.2-1880 ppb.

Isoprene in human breath

Isoprene is another major VOCs in human exhaled breath. Usually, the concentration of isoprene is in the sub-ppm level. In 1984, Denise et cl suggested by experiments that breath isoprene was possibly linked to cholesterol synthesis [10]. Its formation occurs in human body as

a by-product of the biosynthesis of cholesterol. This finding raised the possibility that measurements of breath isoprene might become a noninvasive and simple way for assessing body cholesterol status. The effectiveness of lipid-lowering therapy can also be evaluated by monitoring the concentration of breath isoprene in patients. Nevertheless, though breath isoprene seems to be a promising candidate for breath analysis, there are some factors (age, gender, heart rate, etc.) [11, 12] may affect its concentration in exhale breath and thus influence the accuracy of measurement so that they need to be taken into consideration. Besides, an uniform standard is need for sampling and measurement.

1.2 Chemical sensors

A chemical sensor is a device that "transforms chemical information, ranging from the concentration of a specific sample component to total composition analysis, into an analytically useful signal. The chemical information, mentioned above, may originate from a chemical reaction of the analyte or from a physical property of the system investigated." [13] Based on the working mechanism, chemical sensors can be classified into several groups: electrical sensors, electrochemical sensors, optical sensors, and mass sensitive sensors, etc.

1.3 NO detection by chemical sensors

1.3.1 By chemiresistive sensors

Chemiresistive sensors have been widely used for gas sensing. When analyte molecule interact with the sensing layer, physical or chemical reaction occur and thus change the charge carriers density of the sensing layer, causing a resistance change which can be then detected and recorded by multimeters. For NO detection, many metal oxides have been employer as gas

sensing materials. Some researchers have also investigated the effect of doping or decoration with metals. The following table is a summary of sensing properties of some chemiresistive sensors to NO. Table-1 is a summary of sensing properties of some chemiresistive sensors to NO.

Table-1 Summary of sensing properties of some chemiresistive sensors to NO

Sensing material	Minimum/saturation detection limit (MDL/SDL)	Response/ recovery time	Optimal working temperature	Sensitivity	Ref.
hierarchically porous structured monoclinic WO_3	N/A	response 63 s recovery 223 s	200 ℃	46.2 for 100 ppm NO	[14]
β-WO_3	N/A	response ~ 40 s	180 ℃	13 for 10 ppm NO	[15]
Villi-like monoclinic WO_3	MDL 88 ppt	N/A	200 ℃	278 for 1 ppm NO	[16]
Au/δ-WO_3	MDL 500 ppb	response 15 s recovery 24 s	170 ℃	~55 for 10 ppm NO	[17]
Ag/δ-WO_3	MDL 500 ppb	response <10 s recovery <100 s	170 ℃	~90 for 2 ppm NO	[18]
WO_3/Cr_2O_3 mixture	MDL 18 ppb	N/A	300 ℃	~1.3 for 200 ppb NO	[19]
Pt/In_2O_3-WO_3	MDL 25 ppb	response <20 min recovery <120 min	room temp.	15.2 for 25 ppb NO	[20]

1.3.2 By surface acoustic wave-based sensors

1.3.2.1 Surface acoustic wave (SAW)

J.M. Strutt, Lord Rayleigh, was the first one to discover and introduce surface acoustic wave (SAW). In his paper published in 1885 [21], he described the surface acoustic mode of propagation and predicted its properties. A surface acoustic wave (SAW) can be defined as an acoustic wave moving along the surface of an elastic material while its amplitude usually decays with depth into the substrate exponentially [22]. Rayleigh surface acoustic wave (RSAW) is the main type of the SAWs of importance. It combines longitudinal and transverse motions, resulting in displacements parallel and perpendicular to the surface of substrate. Fig. 1 depicts the particle displacements of Rayleigh wave.

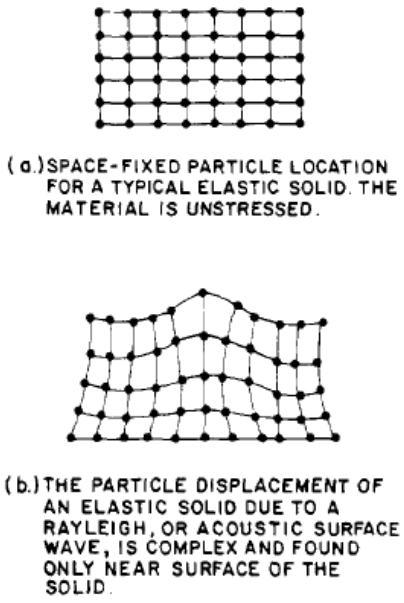

Fig. 1 Rayleigh wave particle displacement. Copied from Ref. [23]

Some major properties of Rayleigh SAW are the following: the penetration depth of the RSAW is ~1 wavelength, so the majority of energy of the wave is localized in the surface region which means that the surface region has a very high energy density; the velocity of RSAW is relatively slow, only ~45% that of P-wave and ~90% that of S-wave [24].

1.3.2.2 Basic principle of operation of SAW-based gas sensor

The first SAW-based device for gas sensing was designed by H. Wohltjen et cl in 1979 [23] and since then, this techniques has been developing fast. The basic principle of how devices of this kind work is quite simple. Typically, a SAW sensor is consist of a piezoelectric substrate, two interdigital transducers (IDTs) deposited on top of the substrate, and a sensing layer deposited on the space that is located between those IDTs [25].

Fig. 2 shows how the surface acoustic wave is generated: The high-frequency electrical signal is applied to the input interdigital transducer (interdigital electrode in Fig. 2), then the surface of the piezoelectric substrate will oscillate due to inverse piezoelectric effect and emit an surface acoustic wave in the exact same frequency with the input electrical signal. This SAW propagating on the surface of substrate then reach to the output IDT and transforms to an electrical signal, while the frequency still the same with the input.

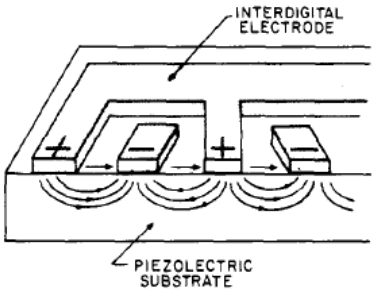

Fig. 2 Interdigital transducer operation. Copied from Ref. [23]

If the sensing layer interacts with analyte molecules from surrounding atmosphere, then its physical or chemical properties will change and thus have an influence on the propagating SAW, causing alterations in the frequency of SAW. These alterations then can be detected by other electronics. Theoretically, though any changes in the physical properties of a sensing layer, due to its interaction with analyte gases, can have influences on the propagation of SAW. However, from the point of view in practical use, only two variations in properties have potentials to be utilized. That is, changes in the mass density of sensing layer, or changes in its electrical conductivity. Only these two variations can cause significant changes in the velocity and attenuation of the SAW and consequently changes in the frequency [26].

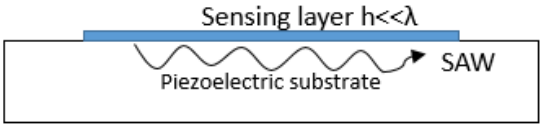

Fig. 3 Schematic of how SAW propagates. Redraw from Ref. [22]

Usually, in practice, two identical acoustic channels are formed on the piezoelectric substrate. One of them is coated with sensing layer (shadow area in Fig. 4) and becomes the measuring channel while the other one uncoated, serving as reference. The reference channel can compensate for small variations of temperature and pressure and thus reduce interference from environment. Both delay lines are placed in the feedback loop of oscillator circuits and the response to the particular gas of the sensing layer is detected as a change in the differential frequency Δf, i.e. the difference between the two oscillator frequencies f and f_0. This whole set up forms the so-called dual-delay line SAW gas sensor.

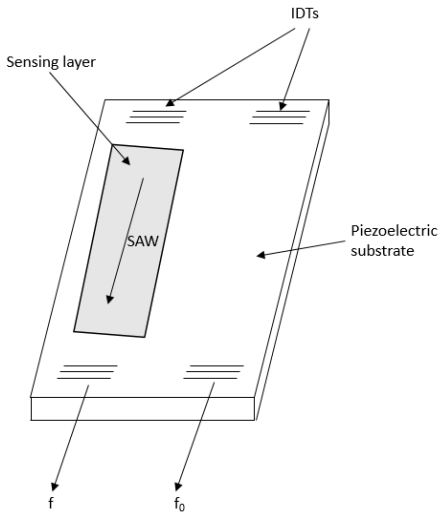

Fig. 4 Schematic of SAW-based gas sensor with dual-delay line. Redraw from Ref. [26]

1.3.2.3 NO sensing properties of SAW-based sensor

Though extensive works have been done to detect NO by other kind of chemical sensors, there are not too many papers about using sensors based on Rayleigh surface acoustic wave. These gas sensors are highly sensitive to trace amount of NO and the most remarkable advantage, compared with most chemiresistive gas sensors, is that some of them can be operated at room temperature, thus significantly reducing energy consumption.

In 1997, J.J. Caron et cl developed a SAW gas sensor to detect NO of low concentration, the sensing material employed in their work was ruthenium-doped tungsten oxide [27]. This Ru-doped WO_3 sensing layer was deposited on a 24-degree rotated quartz substrate by RF sputtering at 500 ℃. In this work, the optimal thickness of the sensing layer was set at 400 Å, along with an optimal operating temperature at 250 ℃, by experiments. These two parameters were chosen to achieve a balance of requirements for high selectivity and short response/recovery time. The sensing tests showed that the SAW sensor had high sensitivity to NO at low concentration (The

change in frequency can reach up to 50 kHz in their work while detection limit of modern electronics is within 1 Hz) and were insensitive to humidity fluctuation or interfering gases like CO, CO_2 and NH_3. The concentration range of NO tested was from 400 ppb to 5 ppm. It was found that the sensor responded in an almost linear line up to 3 ppm, which can be regarded as the saturation detection limit. The minimum detection limit can be as low as 20 ppb by their estimation.

S.H. Wang's research group had published a series of papers about Rayleigh SAW-based nitric oxide gas sensors for room temperature operation. The sensing layers were made of polyaniline/tungsten oxide (PANI/WO_3) or polyaniline/tin oxide (PANI/SnO_2) nanocomposite in their works by a sol-gel method and modifications using copper ion as dopants were also investigated [28-30]

In their first work, PANI/WO_3 composite was employed as sensing material. At a fairly low working temperature (from 24 to 30 ℃), the sensing layer showed good selectivity to NO and was insensitive to interfering gases such as NO_2 or CO_2. The time it took for the sensor to respond to the presence of NO was less than 80 seconds and about a same time was needed for it to recover to the baseline. The sensor was highly sensitive to NO and the estimated minimum detection limit was a little higher than 20 ppb. In their more recent works, copper ions were used as dopants to try to improve the performances of the sensors and hence Cu-doped PANI/SnO_2 or Cu-doped PANI/WO_3 were prepared. For the Cu-doped PANI/SnO_2, the detection limit was about 5 ppb of NO and the frequency response of sensor was almost linear to NO concentration in the range of 10 to 130 ppb. The stability of sensor was also investigated by repeating the sensing test daily for 30 days and comparing the acquired results to those of a fresh sensor. It was found that the differential was negligible, which confirmed that the sensor was stable for a

relatively long period of time and may be suitable for practical use. As for the Cu-doped PANI/WO_3, the minimum detection limit can be even lowered to 1 ppb of NO, however, the response reached to a saturation point when concentration of NO was beyond 70 ppb. The sensitivity of the Cu-doped PANI/WO_3 sensor was the highest among all other composites synthesized and can be more than 400 when exposed to 20 ppb of NO. Table-2 is a summary of the properties of previously mentioned RSAW sensors.

Table-2 Summary of the properties of RSAW sensors

Sensing material	Minimum/saturation detection limit (MDL/SDL)	Response/ recovery time	Optimal working temperature	Sensitivity	Ref.
Ru-doped WO_3	MDL<20 ppb SDL~3 ppm	response 30 s recovery 90 s	250 ℃	~40 for 1 ppm NO	[27]
PANI/WO_3	MDL~23 ppb	20-80 s	room temp.	7.6 for 636 ppb NO	[28]
Cu-doped PANI/SnO_2	MDL~5 ppb	N/A	room temp.	17.7 for 30 ppb NO	[29]
Cu-doped PANI/WO_3	SDL~70 ppb	response 97 s recovery 37s	room temp.	430 for 20 ppb NO	[30]

1.3.3 By potentiometric sensors

The working mechanism of a potentiometric sensor is quite simple: The sensor consists of two electrodes, one is sensing electrode and the other is reference electrode. Upon exposure to

analyte gas, the sensing electrode will react with the gas and result in a potential change, and the potential difference between sensing electrode and reference electrode can be measured, thus detecting the existence of the analyte and measuring its concentration. Fig. 5 is a schematic of a potentiometric sensor.

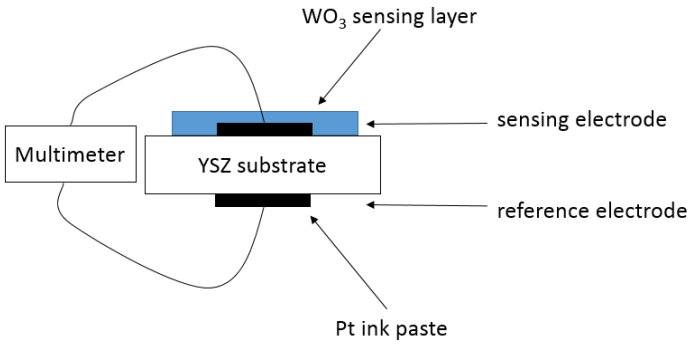

Fig. 5 Redrawn schematic of the potentiometric sensor described in Ref. [31]

Y. Tu et cl synthesized WO_3 nanoplates by microwave intercalation and they compared their sensing properties to WO_3 nanoparticals [31]. In this work, YSZ was used as solid state electrolyte. WO_3 was deposited on YSZ as sensing electrode and Pt was printed on the other side of YSZ to form a reference electrode. The sensing test was carried out at 500 ℃ with a NO concentration range of 100-1000 ppm. S.P. Mondal et cl developed a highly sensitive potentiometric NO sensor by combining a series of identical WO_3-based sensors together [32]. In their works, it is proven that adding identical sensors in series can reduce the detection limit. One of their previous work showed that a 3-sensor array can lower the detection limit of NO to low ppm levels [33] while in Ref. [32], the detection limit was down to ~20 ppb by a 20-sensor-array at 425 ℃.

1.3.4 By optical absorbance sensor

An electrochromic device was developed by researchers [34]. In this work, a 300-nm-thick amorphous WO_3 thin film was deposited on a silicon substrate by sputtering. The WO_3 film was then integrated with a pin structure photodetector. A gold layer was coated on the WO_3 film. Fig. 6 is the schematic of the sensor. Its working mechanism can be briefly summarized as following:

The analyte gas, NO, was ionized by the gold film. WO_3 sensing layer will react with these ions and transfer its color from transparency to blue. The color change will degrade the absorption of incident light that had a wavelength longer than blue, thus decreasing the photocurrent generated by the photodetector. Consequently, the existence of NO can be detected.

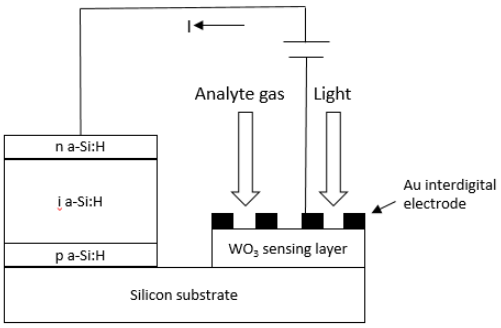

Fig. 6 Redrawn schematic of the WO_3/pin structure sensor described in Ref. [34]

The minimum detection limit of this sensor was about 1 ppm NO, with a sensitivity of 1.02. The sensitivity will increase as the concentration of NO getting higher and reach to saturation when concentration was beyond 150 ppm. The response time was quite short (within 10 s), whereas the recovery time was about 2 min.

1.4 Acetone detection by chemical sensors

1.4.1 WO_3-based chemical sensors

WO_3 in various phases has been widely used as sensing materials on gas sensors. There are also plenty of works about the methods to improve the properties and performances of WO_3-based sensors, either by metal catalyst or doping.

Crystal structures of WO_3 are quite diverse, thus WO_3 can exist in many different phases, including some stable phases such as monoclinic phase (ε-WO_3, γ-WO_3), triclinic phase (δ-WO_3), orthorhombic phase (β-WO_3), tetragonal phase (α-WO_3), and metastable phase like hexagonal phase (h-WO_3). For acetone detection, γ-WO_3, ε-WO_3, δ-WO_3 et cl have been studied. J.C. Shi et cl [35] have synthesized γ-WO_3 by a sol-gel method. The minimum detection limit was down to 50 ppb at a working temperature of 300 ℃. The sensitivity was 3.37 for 900 ppb acetone. D.L. Chen et cl [36] acquired δ-WO_3 nanoplates by a topochemical conversion from tungstate-based inorganic-organic hybrid nanobelts. They have tested the sensing properties towards 2-1000 ppm acetone at 300 ℃ and found that the performance of WO_3 nanoplates was better than WO_3 nanoparticles.

One possible method to improve the performance is adding catalyst to functionalize the WO_3. Some noble metals like platinum, gold or palladium have been added to decorate WO_3 [37, 38] In Ref. [38], WO_3 decorated with both Pd and Au showed ~2 fold stronger response to acetone than those pure WO_3 sensors. Graphene and graphene oxide have also been introduced to functionalize WO_3 [39], the detection limit was as low as 100, with a less than 10 s response time.

Doping is another way that attractive a lot of attentions by researchers. M. Righettoni et cl published a series of papers discussing Si- or SiO_2-doped ε-WO_3 [40-42] and their properties. In their works, the minimum concentration of acetone that can be detected was 20 ppb, which has been the lowest value reported so far. WO_3 doped by Cu, carbon and Cr_2O_3 have also been reported and the sensors had different performances towards acetone [43-45].

1.4.2 Other metal oxides used as sensing materials for acetone detection

1.4.2.1 ZnO

Works regarding to the detection of acetone of various concentrations by ZnO-based sensors are published by many researchers and quite a few of them show that ZnO exhibits good sensitivity to the target gas, acetone. The structures of ZnO employed in these works are quite diverse and they affect the sensing properties (sensitivity, response/recovery time, etc.) significantly.

The concentration of breath acetone for healthy person lies in the sub-ppm level, while that value for patients with diabetes is usually a bit higher, typically a few ppm. Therefore, the detection limit of acetone sensors intended for breath analysis should be as low as possible.

Q. Jia et cl synthesized dandelion-shaped hierarchical ZnO by a solvothermal method and the products were hexagonal phase [46]. The sensing properties of ZnO sensor to acetone were acquired and the concentration range of analyte was from 250 ppb to 100 ppm. Also, the influence of working temperature on performances were taken into consideration. In their work, the optimal working temperature of sensor was found to be at around 230 ℃, when exposed to 100 ppm of acetone.

From the result, it can be concluded that the minimum detection limit can be as low as 0.25 ppm, which was in the range of breath acetone, confirming that the sensor had a potential for breath analysis. When concentration was beyond 50 ppm, the sensor reached a saturation point. Though the calculate sensitivity may still be increasing, it should be noted that the resistance had a baseline shift which cannot be ignored. This phenomenon was very common for semiconductor sensors and may imply that this sensor need a further stabilization in order for practical use. In conclusion, this ZnO sensor showed good sensitivity to acetone (~1.2 for 0.25 ppm acetone and ~2 for 2 ppm acetone), selective (insensitive to interfering gases like NH_3, methanol, benzene and xylene) and a short response time (~3 s).

1.4.2.2 SnO_2

SnO_2 is a n-type semiconductor with a wide band gap and it shows great potential to be used for gas sensors because it is inexpensive, easy to be processed and non-toxic [47]. L. Cheng et cl synthesized SnO_2 hollow nanofibers with porous surface by electrospinning and improved its sensing performance to acetone by doping with yttrium ions [48]. In their work, the diameter of nanofibers increase when yttrium was introduced into the products and it is related to the content of Y.

In the gas sensing test, an optimal working temperature, at 300 ℃, was found for those Y-doped SnO_2 sensors, while for the pure SnO_2 sensor, its response (sensitivity) keeps at a relatively low level compared to those doped samples. Of all Y-doped SnO_2 sensors (content of Y were 0.1%, 0.4% and 0.7%, respectively), the one with a 0.4% content of yttrium exhibited the best sensing properties. The sensitivity were 12 for 50 ppm acetone and can detect the presence of acetone down to a concentration of 20 ppm. The stability was also investigated, in a 60-day

cycle, the response of SnO_2 sensor to 500 ppm acetone was consistent and almost no significant fluctuation was observed.

1.4.2.3 InN

K.W. Kao et cl have developed a InN gas sensor which was able to detect trace amount of acetone and modification with Platinum as catalyst was also reported [49] In this work, sensing properties of bare InN and Pt-coated InN were evaluated. For the bare InN sensor, though it exhibited high sensitivity to acetone, the response time and recovery time, 1260 s and 3740 s respectively for 10 ppm acetone at 200 ℃, were too long. Consequently, Pt was employed as catalyst to shorten the response time. And it was shown in the result that under an identical circumstance, the response time and recovery time were reduced by more than 8 fold and an enhanced performance to acetone was achieved as well. The Pt-InN sensor showed a sensitivity of 28.7 for 10 ppm acetone at an optimal working temperature of 200 ℃. It can respond to acetone in 150 s and recover to the initial status in 2000 s.

Table-3 Summary of performances of some acetone sensors

Sensing material	Minimum/saturation detection limit (MDL/SDL)	Response/ recovery time	Optimal working temperature	Sensitivity	Ref.
SiO_2-doped WO_3	MDL 20 ppb	N/A	400 ℃	4.6 for 600 ppb acetone	[40]
Si-doped WO_3	MDL 20 ppb	response 10-15 s recovery 35-70 s	350 ℃	~2.8 for 500 ppb acetone	[41]
Cr_2O_3-doped WO_3	MDL 500 ppb	N/A	320 ℃	8.91 for 20 ppm acetone	[45]
h-ZnO	MDL 250 ppb	3 s	230 ℃	1.16 for 250 ppb acetone	[46]
ZnO-CuO	MDL 100 ppb	<15 s	310 ℃	~2 for 1ppm acetone	[50]
Y-doped SnO_2	MDL 20 ppm SDL 8000 ppm	response 9-30 s recovery 6-9 s	300 ℃	4 for 20 ppm acetone	[48]
Pt-InN	MDL 400 ppb	response 150 s recovery 2000 s	200 ℃	28.7 for 10 ppm acetone	[49]

Sensing material	Minimum/saturation detection limit (MDL/SDL)	Response/ recovery time	Optimal working temperature	Sensitivity	Ref.
δ-WO_3	MDL 2 ppm	response 3-10 s recovery 12 s	300 ℃	~3.5 for 2 ppm acetone	[36]
γ-WO_3	MDL 50 ppb	<30 s	300 ℃	3.37 for 0.9 ppm acetone	[35]
Pt/WO_3	MDL 120 ppb	N/A	350 ℃	4.11 for 2 ppm acetone	[37]
Graphene/WO_3	MDL 100 ppb	response<15 s recovery<30 s	300 ℃	1.7 for 100 ppb acetone	[39]
Au,Pd/WO_3	MDL<200 ppm	~100 s	300 ℃	~100 for 200 ppm acetone	[38]
Cu-doped WO_3	MDL 250 ppb	response 5 s recovery 20 s	300 ℃	1.57 for 250 ppb acetone	[43]
C-doped WO_3	MDL 200 ppb	response 3-9 s recovery 6-12 s	300 ℃	~2 for 200 ppb acetone	[44]

Chapter 2 Experimental details

In this chapter, details about sensor preparation and sensing test set up will be introduced.

2.1 WO_3 powder synthesis by flame spray pyrolysis

The sensing materials used were tungsten trioxide synthesized by other group members. The method was flame spray pyrolysis, using a nanopowder synthesis system in our lab (Tethis nps10). Typically, there are three main parts of a FSP system: an atomizer, a burner and a collector. In the atomizer, droplets of liquid precursor are formed and then these droplets are mixed with carrier gas and are transported to the substrate. In the burner, fuel and oxygen are mixed with the droplets of precursor to form spray which will be ignited then. In the collector, final products will be collected from the substrate of filter. Compared with other methods, one of the advantages of FSP method is that the flame is self-sustaining so that no external flame source is needed. Some other advantages of FSP include high temperature flame, less consumption of precursor and large temperature gradients [51].

WO_3 powders were synthesized and provided by my colleague, Wenling Liao. The procedures for synthesis of powders are as follows: 30 mL of precursor for each different precursor solutions. The sample used for sensing test in this work was synthesized with the following precursor solution, shown in Table a. The flame consisted of 1.5 sl/min of methane and 3.2 sl/min of oxygen. 5 sl/min of oxygen was fed into the reactor, serving as dispersion gas. The precursor flow rate was set at 5 ml/min. The final products were collected on the glass fiber filters. The as-synthesized powders were greyish green in color.

Table-4 Recipe of precursor solution

Sample Number	Solute	Solvent	Concentration
Labelled as "Sp2"	Tungsten (VI) isopropoxide	Isopropanol	0.22 M

2.2 Sensor preparation

The 3x3 mm2 alumina substrates coated with platinum interdigitated electrodes were first sonicated in ethanol for 15 min to clean up the surface and remove oxide layer. Then gold wires (99.95%, 0.1mm in dia., Alfa Aesar) were welded onto the substrate with a welding machine (Unibond Ⅱ, Unitek Equipment). To prepare the gas sensor, the as-synthesized WO_3 powders were dissolved in ethanol and the solution was sonicated for 15 min. One drop of the suspension was then dripped onto the substrate and the substrate was dried at ~100 ℃ for 2 min to remove the ethanol. Such process was repeated for 10 times and the sensing materials was deposited on the substrate uniformly. The drop-coated substrate was heat treated in a tube furnace (Lindberg/Blue M) at 500 ℃ for 8 h to stabilize the sensor. The color of heat-treated powder changed to yellowish green.

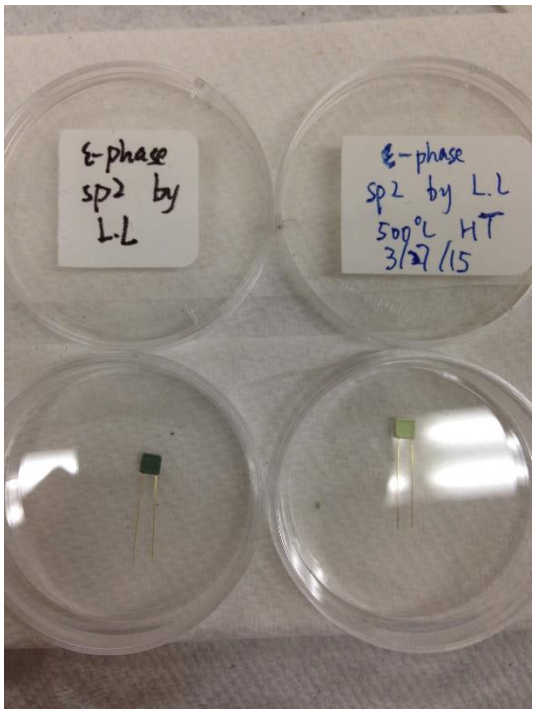

Fig. 7 Sensor prepared with Wenling's powders
Greyish green one: as-synthesized sample
Yellowish green one: sample heat treated at 500 ℃ for 8 h

2.3 Gas sensing test setup

The drop-coated sensor was put in a quartz tube and was connected to the measuring circuit with gold wire welded on the substrate. Then the tube was put into the tube furnace and the resistance of the sensor was recorded by a computer-controlled multimeter (34401A 6.5 digit multimeter). The real-time change of resistance of the sensor can be monitored by software.

The background gases were synthetic air (80% nitrogen, 20% oxygen, Praxair Inc.) and the analyte gases were acetone and isoprene. The concentration of analyte gases in the mixture was controlled by altering the flow rates of analyte gases. The flow rates were controlled by a mass flow controller (1479 MKS) in the unit of stand cubic centimeter per minute (sccm) and the

value was monitored by a 4-channel readout (MKS Type247). Analyte gases include: acetone, isoprene and NO (The concentration for all kind of analyte gases is 10 ppm in nitrogen, produced by Global Calibration Gases LLC). Fig. 8 is a schematic of the sensing test setup.

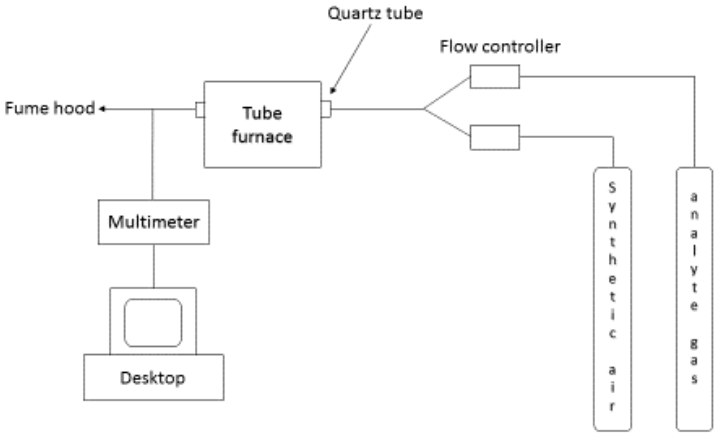

Fig. 8 Schematic of the sensing test setup

Chapter 3 Experiment results

In Wenling's thesis [52], it was stated that γ-phase WO_3 and ε-phase WO_3 coexisted in the as-synthesized powder. The γ-phase was the predominant one while there was almost no ε-phase in the sample, according to Raman spectra she acquired. However, after a heat treatment for 8 h at 500 ℃, the content of ε-phase increased a lot and ε-phase and γ-phase shared an approximately same percentage in the sample. This was confirmed by the Raman spectra of heat-treated sample, the intensities of characteristic peaks of ε-phase (at 688 cm-1) and γ-phase (at 715 cm-1) were about the same (Lisheng Wang's dissertation [53]).

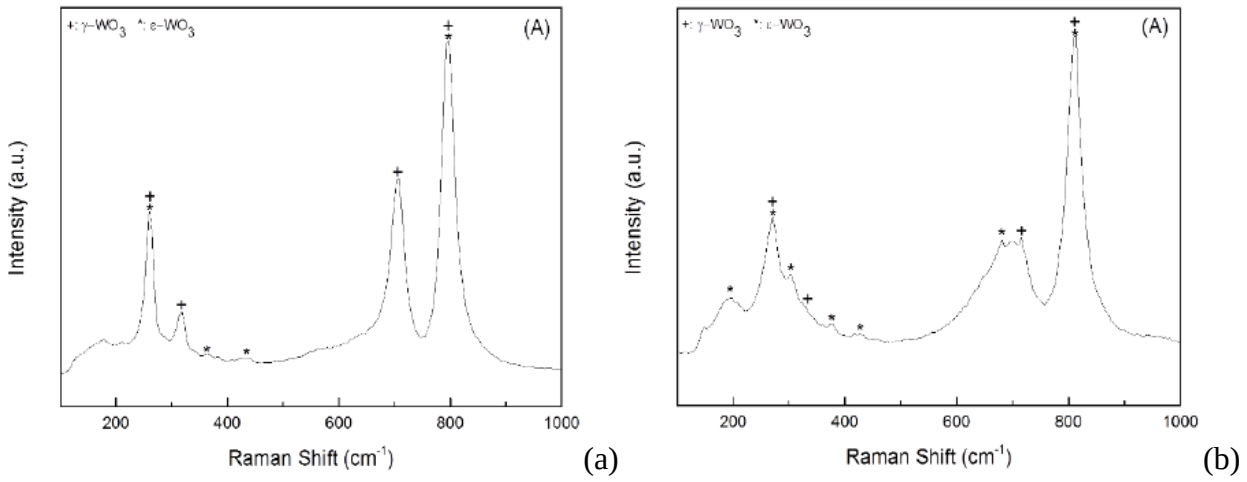

Fig. 9 Raman spectra of (a) as-synthesized WO_3 and (b) heat-treated WO_3
Copied from Wenling Liao's thesis

Based on the previous works by other group members, it was concluded that ε-phase WO_3 exhibit selective detection on acetone. Therefore, sensing tests towards acetone of various concentrations samples have been conducted and the results are presented as following.

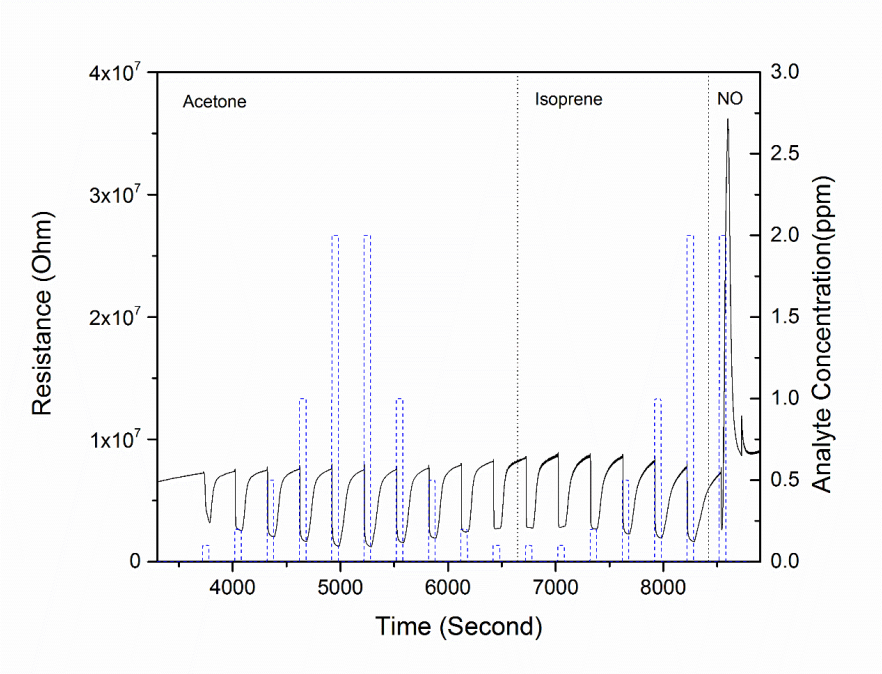

Fig. 10 Sensing response of sensor to acetone, isoprene and NO at 300 ℃. 1min for each pulse of analyte gas

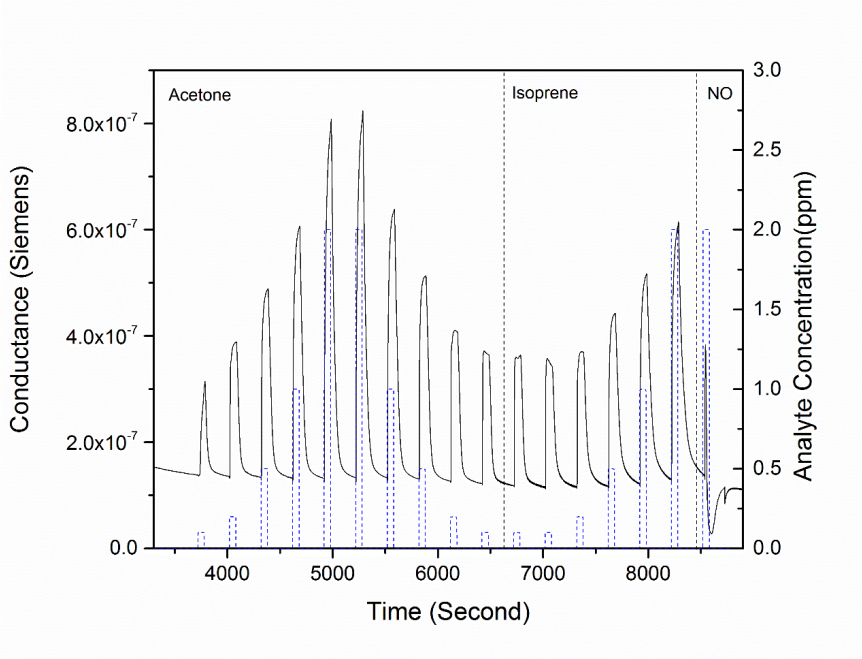

Fig. 11 Sensing response of sensor at 300 ℃: Conductance vs. Time

Fig. 10 shows the sensing result of the sensor at a working temperature of 300 ℃, the analyte gases tested are acetone, isoprene and nitric oxide. The duration of each injection of gas is 1 min and a 4 min is allowed for the sensor to recover. As is shown in the figure, when acetone or isoprene are introduced, the resistance of sensor decreases as expected due to its properties (When n-type semiconductor interacts with reducing gases, the concentration of its major charge carrier, electrons, increases because gas molecules will release electrons when redox reactions happen.) When NO is injected into the tube, the resistance increases because NO is a kind of oxidizing gases. The responses to different kinds of analyte gases confirm that it is a n-type semiconductor gas sensor. In Fig. 11, resistance has been converted into conductance and the equation employed is:

$$G=1/R,$$

where G is conductance and R is resistance.

In Fig. 10 it might be difficult to observe the resistance changes and compare the performances of the sensor to acetone or isoprene, because resistance cannot be lower than zero. Hence, Fig. 11 is plotted and it is just a mathematical conversion. It might be easier to notice that at the same concentration, especially in the range of 0.5-2 ppm, the sensor is more selective to acetone than isoprene

Usually, four main parameters are used for the evaluation of the performances of a sensor, namely: sensitivity, selectivity, response/recovery time and stability. For a chemiresistive gas sensor, sensitivity can be defined as the magnitude of the resistance change of the sensor when exposed to analyte gases. In this work, sensitivity is defined as the following equation:

$$\text{Sensitivity (S)} = R_a/R_g \text{ (when } R_a>R_g) \text{ or } R_g/R_a \text{ (when } R_a<R_g),$$

where R_a is the resistance when only background gases are introduced,

R_g is the resistance when analyte gases are introduced

The selectivity is referred to the ability of a gas sensor to separate a specific gas from other interfering gases. An ideal gas sensor should be sensitive to only one particular gas while insensitive to the others.

Response/recovery time is about how fast the gas sensor respond to the concentration change of the analyte gas. In this work, response time is defined as the time it takes for the resistance to go from R_a to $90\%R_g+10\%R_a$, and recovery time is the time it takes for the resistance goes back from R_g to $10\%R_g+90\%R_a$.

Based on Fig. 10, we can calculate the sensitivity and response/recovery time, Table-5. Table-6 are the summaries of the performances of the sensor to acetone and isoprene, respectively. Fig. 12 is a plot of sensitivity vs. analyte concentration. The baseline has a shift of less than 1.4 MΩ (from 7.23 MΩ to 8.60 MΩ) while the minimum change in resistance is ~4 MΩ.

Table-5 Sensing performance of sensor towards acetone at 300 ℃

Concentration/ppm	Sensitivity	Response Time/s	Recovery Time/s
0.1	2.59	4.7	82.2
0.2	3.04	6.7	87.8
0.5	3.82	9.5	112.9
1.0	4.67	11.2	120.8

2.0	5.99	12.5	137.4

Table-6 Sensing performance of sensor towards isoprene at 300 ℃

Concentration/ppm	Sensitivity	Response Time/s	Recovery Time/s
0.1	2.98	5.9	127.2
0.2	3.19	5.9	148.5
0.5	3.83	10.5	202.4
1.0	4.28	10.3	214.2
2.0	4.73	11.2	231.7

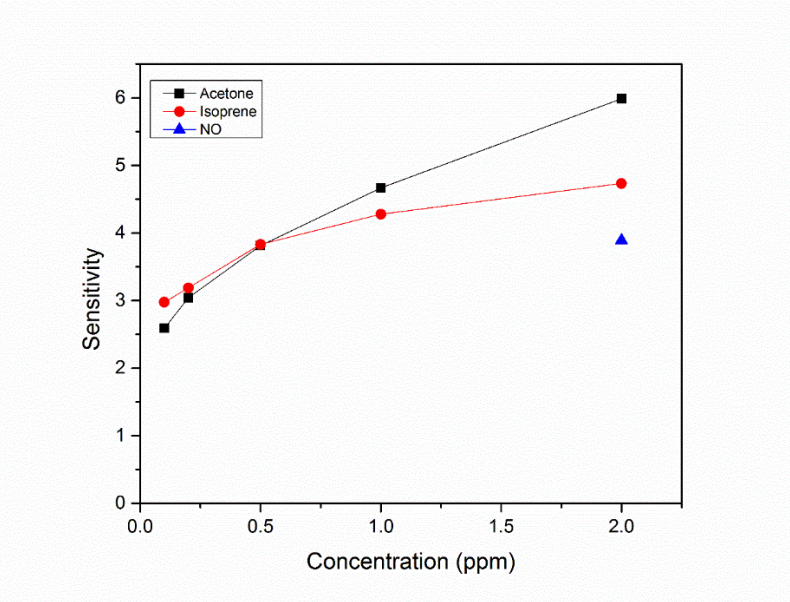

Fig. 12 Sensitivity curve to different concentrations of acetone and isoprene at 300 ℃

It can be seen in Table-5 and Table-6 that the response time of the sensor is rather short and is within a few seconds no matter what kind of analyte gases have been injected, indicating that it react to the target gases almost immediately. Nevertheless, the recovery time is relatively longer and can be up to near several minutes. In Fig. 10, it can be observed that a few seconds after the injection of analyte gases, the curve reach a steady state and the resistance hardly change. This phenomenon indicates that the duration of gas injection may be shortened to like 30 seconds or even less, which is very important for practical use since a single breath cannot last for minutes.

It should be noted that at same concentration, the recovery time of the sensor to acetone is much less than it is to isoprene and it may be concluded that the sensor is more suitable to be applied to acetone detection. Besides, it should be noted that while the concentration of analyte gases increasing, it takes a longer time for the sensor to recover the initial status, which is as expected.

In Fig. 12, it can be seen that the sensor is more sensitive to acetone when concentration of analyte is beyond 0.5 ppm, while at lower concentration, it is more sensitive to isoprene. Also, it exhibits property of NO detection to some extent. A possible reason may be that γ-phase WO_3 and ε-phase WO_3 coexist in the powder deposited on the substrate. As is mentioned above, only ε-phase is the desired phase for acetone detection while γ-phase is considered to be NO sensitive. Therefore, a possible way to improve the performance of the sensor for acetone detection is that eliminating γ-phase by methods like heat treatment.

Our former group member, Lisheng Wang, had carried out similar gas sensing tests towards acetone and isoprene. In his work, the ε-phase to γ-phase WO_3 ratio was 31.6% to 68.4%，

the working temperature was 350 ℃. At such condition, his sensor showed comparable sensitivity towards isoprene (4.8 at 1 ppm of isoprene) than acetone (~4 at 1ppm of acetone). Compared with his work, the sensitivities to isoprene and acetone in this work (300 ℃ working temperature, ~50% ε-phase WO_3 ratio) are 4.28 and 4.67, respectively， which is consistent with the presence of γ-phase favoring adsorption of hydrocarbons, this reducing ε-phase selectivity to acetone..

Sensing response at 250 ℃

As demonstrated in many literatures, the working temperature has a great influence on the sensing response of the sensors. Therefore, gas sensing tests at 250 ℃ was carried out. The injection time is 30 s for each concentration. Fig. 13 shows the result.

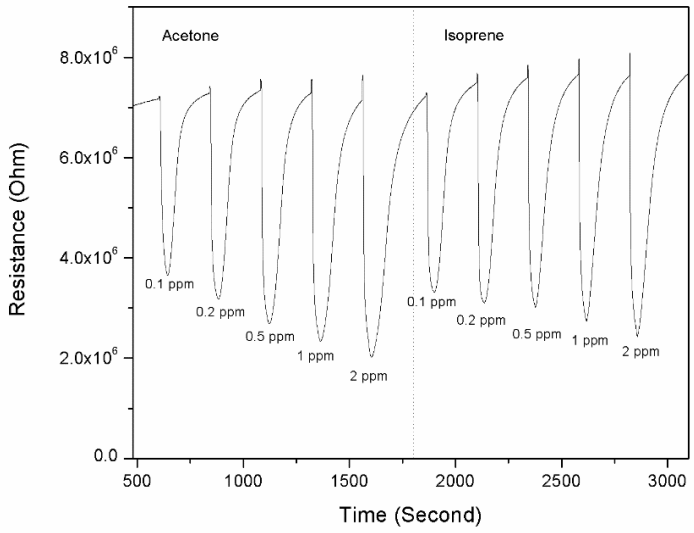

Fig. 13 Sensing response to acetone and isoprene at 250 ℃

Using the equation, sensitivities to acetone and isoprene at different concentrations have been calculated and is shown in Table-7.

Table-7 Sensitivities calculated to acetone and isoprene at 250 ℃

Concentration/ppm	Sensitivity to acetone	Sensitivity to isoprene
0.1	1.89	2.15
0.2	2.19	2.38
0.5	2.57	2.44
1.0	2.85	2.66
2.0	3.11	2.91

From the above results, the sensitivities of this sensor to acetone is lower than that of isoprene at relatively lower concentration (< 0.5 ppm). When the concentration of analyte is beyond 0.5 ppm, the sensor is more sensitive to acetone. This result is consistent with the result at 300 ℃. If we focus on the absolute value, the values at 250 ℃ are lower than those at 300 ℃. Therefore, comparing results at 250 and 300 ℃, 300 ℃ may be better as working temperature for this sensor.

Chapter 4 Future work

As is mentioned in the previous chapter, the WO_3 powders used for sensing test consist both γ-phase and ε-phase and actually, γ-phase is the predominant phase existing. Therefore, developing a proper method, either by heat treatment or modification of processing, to rule out γ-phase WO_3 in the powder might be able to improve the sensing properties to the target analyte, acetone. Working environment like operating temperature may also effect the properties. Sensing tests conducted under different operating temperature can be carried out to evaluate the effects, thus enabling us to find out an optimal temperature. Long-term stability should also be investigated for practical use.

Reference

[1] Wolfram Miekisch, Jochen K. Schubert, Gabriele F.E. Noeldge-Schomburg, *Diagnostic potential of breath analysis—focus on volatile organic compounds*, Clinica Chimica Acta 347 (2004) 25–39

[2] Biomaker Definitions Working Group, *Biomarkers and surrogate endpoints: Preferred definitions and conceptual framework*, CLINICAL PHARMACOLOGY & THERAPEUTICS, Volume 69, Number 3, 2001

[3] M.G. Zhou, Y. Liu, Y.X. Duan, *Breath biomarkers in diagnosis of pulmonary diseases*, Clinica Chimica Acta 413 (2012) 1770-1780

[4] Dupont. LJ et cl, *Prospective evaluation of the accuracy of exhaled nitric oxide for the diagnosis of asthma*. Am. J. Respir. Crit. Care. Med, 1999, 159:A8631-A

[5] Dupont. LJ et cl, *Prospective evaluation of the validity of exhaled nitric oxide for diagnosis of asthma*, Chest. 2003; 123:751-6

[6] L. Pauling, A.B. Robinson et cl, *Quantitative Analysis of Urine Vapor and Breath by Gas-Liquid Partition Chromatography*, Proc. Nat. Acad. Sci. USA Vol. 68, No. 10, pp. 2374-2376, October 1971

[7] Michael Phillipsa, Jolanta Herrerab, Sunithi Krishnanb, Mooena Zainb, Joel Greenberg , Renee N. Cataneo, *Variation in volatile organic compounds in the breath of normal humans*, Journal of Chromatography B, 729 (1999) 75–88

[8] C.H. Dent et cl, *Determination of acetone in human breath by gas chromatography-mass spectrometry and solid –phase microextraction with on-fiber derivation*. J. Chromatogr. B, 2004/ 810(2): 269-275

[9] Jill D. Fenske, Suzanne E. Paulson, *Human Breath Emissions of VOCs*, ISSN 1047-3289 J. Air & Waste Manage. Assoc. 49:594-598

[10] Deneris ES, Stein RA, and Mead JF. *In vitro biosynthesis of isoprene from mevalonate utilizing a rat liver cytosolic fraction*. Biochem Biophys Res Commun 123: 691–696, 1984.

[11] Frank. Cikach, Raed. Dweik, *Cardiovascular Biomarkers in Exhaled Breath*, Progress in Cardiovascular Disease 55 (2012) 34-43

[12] Thomas Karl, Peter Prazeller et cl, *Human breath isoprene and its relation to blood cholesterol levels: new measurements and modeling*, J. appl. Physiol 91: 762-770, 2001

[13] A.Hulanicki, et cl, *CHEMICAL SENSORS DEFINITIONS AND CLASSIFICATION*, Pure&App/. Chern., Vol. 63, No. 9, pp. 1247-1250, 1991.

[14] Xiao-Xue Wang, Kuan Tian, *Bio-templated fabrication of hierarchically porous WO_3 microspheres from lotus pollens for NO gas sensing at low temperatures*, RSC Adv., 2015, 5, 29428

[15] D. Manno, A. Serra, M. Di Giulio et cl, *Physical and structural characterization of tungsten oxide thin films for NO gas detection*, Thin Solid Films 324 _1998. 44–51

[16] Hi Gyu Moon, You Rim Choi et cl, *Extremely Sensitive and Selective NO Probe Based on Villi-like WO_3 Nanostructures for Application to Exhaled Breath Analyzers*, ACS Appl. Mater. Interfaces 2013, 5, 10591−10596

[17] Li Yin, Deliang Chen et cl, *Enhanced selective response to nitric oxide (NO) of Au-modified tungsten trioxide nanoplates*, Materials Chemistry and Physics 143 (2013) 461-469

[18] Deliang Chen, Li Yin et cl, *Low-temperature and highly selective NO-sensing performance of WO_3 nanoplates decorated with silver nanoparticles*, Sensors and Actuators B 185 (2013) 445–455

[19] Chenhu Sun, G. Maduraiveeran, Prabir Dutta, *Nitric oxide sensors using combination of p- and n-type semiconducting oxides and its application for detecting NO in human breath*, Sensors and Actuators B 186 (2013) 117-125

[20] B.Chang, Chen-Yang Wang et cl, *Evaluation of Pt/In_2O_3–WO_3 nano powder ultra-trace level NO gas sensor*, Journal of the Taiwan Institute of Chemical Engineers 45 (2014) 1056–1064

[21] Lord Rayleigh, *On wave propagating along the plane surface of an elastic solid*, Proc. London. Math. Soc. (1885) 17

[22] W.P. Jakubik, *Surface acoustic wave-based gas sensors*, Thin Solid Films 520 (2011) 986-993

[23] Henry Wohltjen, Raymond Dessy, *Surface Acoustic Wave Probe for Chemical Analysis. I. Introduction and Instrument Description*, ANALYTICAL CHEMISTRY, VOL. 51, NO. 9, AUGUST 1979

[24] Telford, William Murray; Geldart, L. P.; Robert E. Sheriff (1990). *Applied geophysics*. Cambridge University Press. p. 149. ISBN 978-0-521-33938-4

[25] Mar á-Isabel Rocha-Gaso, Carmen March-Iborra, Ángel Montoya Baides, Antonio Arnau-Vives, *Surface Generated Acoustic Wave Biosensors for the Detection of Pathogens: A Review*, Sensors 2009, 9, 5740-5769

[26] Marian Urbańczyk, Tadeusz Pustelny, *The Application of Surface Acoustic Waves in Surface Semiconductor Investigations and Gas Sensor Chapter 5*, DOI:10.5772/53717

[27] Joshua J. Caron, Thomas D. Kenny, L. Jay LeGore, Derek G. Libby, Carl J. Freeman, John F. Vetelino, *A Surface Acoustic Wave Nitric Oxide Sensor*, 1997 IEEE INTERNATIONAL FREQUENCY CONTROSLY MPOSIUM

[28] Shih-Han Wang, Shih-Hao Kuo, Chi-Yen Shen, *A nitric oxide gas sensor based on Rayleigh surface acoustic wave resonator for room temperature operation*, Sensors and Actuators B 156 (2011) 668–672

[29] Shih-Han Wang, Chi-Yen Shen, Hsiang-Min Huang, Yi-Cheng Shih, *Rayleigh surface acoustic wave sensor for ppb-level nitric oxide gas sensing*, Sensors and Actuators A 216 (2014) 237–242

[30] Shih-Han Wang, Chi-Yen Shen, Jian-Ming Su, Shiang-Wen Chang, *A Room Temperature Nitric Oxide Gas Sensor Based on a Copper-Ion-Doped Polyaniline/Tungsten Oxide Nanocomposite*, Sensors 2015, 15, 7084-7095; doi:10.3390/s150407084

[31] Y. Tu, Q. Li et cl, *Microwave Intercalation Synthesis of WO_3 Nanoplates and Their NO-Sensing Properties*, JMEPEG (2015) 24:274–279

[32] S.P.Mondal, et cl, *Development of high sensitivity potentiometric NO_x sensor and its application to breath analysis*, Sensors and Actuators B 158 (2011) 292-298

[33] J.C. Yang, P.K. Dutta et cl, *Promoting selectivity and sensitivity for a high temperature YSZ-based electrochemical total NO_x sensor by using a Pt-loaded zeolite Y filter*, Sens. Actuators B 125 (2007) 30-30

[34] Jyh-Jier Ho, *Novel nitrogen monoxides (NO) gas sensors integrated with tungsten trioxide (WO_3)/pin structure for room temperature operation*, Solid-State Electronics 47 (2003) 827–830

[35] Jichao Shi, Gujin Hu Yan Sun et cl, *WO_3 nanocrystals: Synthesis and application in highly sensitive detection of acetone*, Sensors and Actuators B 156 (2011) 820– 824

[36] Deliang Chen, Xianxiang Hou et cl, *Effects of morphologies on acetone-sensing properties of tungsten trioxide nanocrystals*, Sensors and Actuators B 153 (2011) 373–381

[37] Seon-Jin Choi, Inkun Lee, Bong-Hoon Jang et cl, *Selective Diagnosis of Diabetes Using Pt-Functionalized WO_3 Hemitube Networks As a Sensing Layer of Acetone in Exhaled Breath*, dx.doi.org/10.1021/ac303148a | Anal. Chem. 2013, 85, 1792−1796

[38] Soohyun Kim, Sunghoon Park, Suyoung Park, Chongmu Lee, *Acetone sensing of Au and Pd-decorated WO_3 nanorod sensors*, Sensors and Actuators B 209 (2015) 180–185

[39] Seon-Jin Choi, Franz Fuchs, Renaud Demadrille, *Fast Responding Exhaled-Breath Sensors Using WO_3 Hemitubes Functionalized by Graphene-Based Electronic Sensitizers for Diagnosis of Diseases*, dx.doi.org/10.1021/am501394r | ACS Appl. Mater. Interfaces 2014, 6, 9061−9070

[40] M. Righettoni, A. Tricoli, and S.E. Pratsinis, *Thermally Stable, Silica-Doped ε-WO_3 for Sensing of Acetone in the Human Breath*, Chem. Mater. 2010, 22, 3152–3157 DOI:10.1021/cm1001576

[41] Marco Righettoni, Antonio Tricoli, Samuel Gass et cl, *Breath acetone monitoring by portable Si:WO_3 gas sensors*, Analytica Chimica Acta 738 (2012) 69–75

[42] M. Righettoni et cl, *Si:WO_3 Sensors for Highly Selective Detection of Acetone for Easy Diagnosis of Diabetes by Breath Analysis*, Anal. Chem. 2010, 82, 3581-3587

[43] Xue Bai, Huiming Ji, Peng Gao, Ying Zhang, Xiaohong Sun, *Morphology, phase structure and acetone sensitive properties of copper-doped tungsten oxide sensors*, Sensors and Actuators B 193 (2014) 100– 106

[44] Teng Xiao, Xiu-Yue Wang, Zhi-Hua Zhao, *Highly sensitive and selective acetone sensor based on C-doped WO_3 for potential diagnosis of diabetes mellitus*, Sensors and Actuators B 199 (2014) 210–219

[45] Peng Gao, Huiming Ji, Yugui Zhou, Xiaolei Li, *Selective acetone gas sensors using porous WO_3–Cr_2O_3 thin films prepared by sol–gel method*, Thin Solid Films 520 (2012) 3100–3106

[46] Qianqian Jia, Huiming Ji, Ying Zhang, Yalu Chen, Xiaohong Sun, Zhengguo Jin, *Rapid and selective detection of acetone using hierarchical ZnO gassensor for hazardous odor markers application*, Journal of Hazardous Materials 276 (2014) 262–270

[47] Y.L. Wang, X.C. Jiang, Y.N. Xia, *A solution phase precursor route to poly-crystalline SnO_2 nanowires that can be used for gas sensing under ambientconditions*, J. Am. Chem. Soc. 125 (2003) 16176–16177.

[48] L. Cheng et cl, *Highly sensitive acetone sensors based on Y-doped SnO_2 prismatic hollow nanofibers synthesized by electrospinning*, Sensors and Actuators B 200 (2014) 181–190

[49] Kun-Wei Kao, Ming-Che Hsu, Yuh-Hwa Chang, Shangjr Gwo, J. Andrew Yeh, *A Sub-ppm Acetone Gas Sensor for Diabetes Detection Using 10 nm Thick Ultrathin InN FETs*, Sensors 2012, 12, 7157-7168; doi:10.3390/s120607157

[50] Yi Xie, Ruiqing Xing, Qingling Li, Lin Xu, Hongwei Song, *Three-dimensional ordered ZnO–CuO inverse opals toward lowconcentration acetone detection for exhaled breath sensing*, Sensors and Actuators B 211 (2015) 255–262

[51] W.Y. Teoh, R. Amala, L. Madler, *Flame spray pyrolysis: An enabling technology for nanoparticles design and fabrication*, Nanoscale, 2(8), 1324-1347. DOI: 10.1039/c0nr00017e

[52] Wenling Liao's master thesis

[53] Lisheng Wang's Ph.D dissertation